Acta Med. Okayama, 2003
Vol. 57, No. 3, pp. 123-131

Acta Medica Okayama
http://www.lib.okayama-u.ac.jp/www/acta/

Original Article

Radiation Damage to the Normal Monkey Brain: Experimental Study Induced by Interstitial Irradiation

Nobuya Mishima*, Takashi Tamiya, Kengo Matsumoto, Tomohisa Furuta, and Takashi Ohmoto

Department of Neurological Surgery, Okayama University Graduate School of Medicine and Density, Okayama 700-8558, Japan

Radiation damage to normal brain tissue induced by interstitial irradiation with iridium-192 seeds was sequentially evaluated by computed tomography (CT), magnetic resonance imaging (MRI), and histological examination. This study was carried out in 14 mature Japanese monkeys. The experimental area received more than 200-260 Gy of irradiation developed coagulative necrosis. Infiltration of macrophages to the periphery of the necrotic area was seen. In addition, neovascularization, hyalinization of vascular walls, and gliosis were found in the periphery of the area invaded by the macrophages. All sites at which the vascular walls were found to have acute stage fibrinoid necrosis eventually developed coagulative necrosis. The focus of necrosis was detected by MRI starting 1 week after the end of radiation treatment, and the size of the necrotic area did not change for 6 months. The peripheral areas showed clear ring enhancement with contrast material. Edema surrounding the lesions was the most significant 1 week after radiation and was reduced to a minimum level 1 month later. However, the edema then expanded once again and was sustained for as long as 6 months. CT did not provide as clear of a presentation as MRI, but it did reveal similar findings for the most part, and depicted calcification in the necrotic area. This experimental model is considered useful for conducting basic research on brachytherapy, as well as for achieving a better understanding of delayed radiation necrosis.

Key words: interstitial brachytherapy, radiation damage, normal monkey brain, computed tomography (CT), magnetic resonance imaging (MRI)

In many cases, malignant glioma is hard to completely remove by surgery due to both the location of its site of development and its invasive characteristics. Therefore, radiation therapy has great potential to treat residual tumors after an operation, since there are few other available adjuvant therapies effective at treating malignant gliomas. It has already been confirmed that radiotherapy accompanied by surgical operation is more effective than surgery alone, and that an increase in the radiation dose improves the chances of survival. Nonetheless, the prognosis for patients with a malignant glioma is still poor [1]. One of the reasons for this poor prognosis is that ordinary external irradiation cannot provide a sufficient amount of radiation, as it may cause radiation necrosis, brain atrophy, and other postirradiation complications in normal brain tissue surrounding the tumor [2, 3]. Due to the fact that 90% of recurring tumors occur at the primary site of the original tumor [4], high-dose

Received July 17, 2002; accepted January 8, 2003.
*Corresponding author. Phone: +81-86-273-0115; Fax: +81-86-273-0115
E-mail: nobu_mishima@yahoo.co.jp (N. Mishima)

radiation limited to the tumor site can be expected to improve treatment outcomes. Due to recent technological advances, stereotactic radiosurgery (γ-knife, X-knife, cyber-knife) has received a positive clinical evaluation for the treatment of cerebral arteriovenous malformations, vestibular schwannomas, metastatic brain tumors, and other related conditions [5–7]. However, such methods utilize high-dose rate irradiation, which limits the therapeutic area (*i.e.*, volume). In cases of highly infiltrative glioma, especially if the diameter of the glioma exceeds 3 cm, interstitial brachytherapy with continuous low-dose rate irradiation has been considered to be more useful [8].

Use of interstitial irradiation against malignant tumors began in 1901 [2, 9], and the use of brachytherapy against uterine carcinomas, lingual carcinomas, and other cancers has been established as a standard medical treatment [10]. For malignant brain tumors, this type of irradiation treatment has been reported to be effective, in part due to advancements in neuro-imaging technology and stereotactic neurosurgery, and due to improvements in radiation sources [11–13]. Such progress enables more accurate irradiation of tumors, while minimizing the negative effects of irradiation on normal brain tissue. In the Department of Neurological Surgery at Okayama University Hospital, this type of interstitial brachytherapy has been clinically applied against malignant tumors since 1987.

As regards the use of brachytherapy for malignant gliomas, some degree of irradiation of the brain tissue surrounding the target tumor is unavoidable due to infiltration. However, in some cases, this irradiation of the peripheral area causes delayed focal radiation necrosis of normal brain tissue and hence necessitates subsequent necrotomy. Many studies using experimental animals have reported this type of radiation injury to normal tissue caused by interstitial irradiation [15–19]. But the deleterious effects of this mode of irradiation therapy on normal brain tissue have not yet been fully confirmed.

In this study, radiation injury of normal brain tissue was examined with the use of iridium-192 interstitial irradiation of the normal monkey brain. This paper reports the results of neuroradiological and histological examination during the 6-month period following irradiation.

Materials and Methods

Experimental animals and radiation source. Fourteen mature Japanese monkeys (*Macaca fuscata*) weighing 9.5–14.3 kg (average: 12.2 kg) were used in this experiment. Iridium-192 seeds were supplied by the Japan Radioisotope Association (Tokyo, Japan) and the mean radiation intensity of each seed, which was 0.5 mm in outside diameter and 3 mm in length, was 0.779 mCi (0.603–1.056 mCi). In order to gain sufficient dose distribution, 6 seeds were joined vertically and 2 or 3 were joined together, forming seed assembly 18 mm long and 10.85 to 13.35 mCi radiation intensity. The dose calculation was carried out by Toshiba Treatment Planning System, Tosplan TRP01A. The examination was performed according to Okayama University Medical School's Animal Experiment Guide.

Interstitial Irradiation. As a preanesthetic, the monkeys received atropin sulfate (0.02 mg/kg, i.m.), and then were given general anesthesia of ketamine hydrochloride (10 mg/kg, i.m.). After their heads were fixed to a stereotactic frame for the brain, a small craniotomy was performed on the right parietal region (8 mm anterior to the external auditory meatus, 13 mm lateral from the midline) and the dura matter was incised under aseptic conditions. Then, using stereotactic guidance, a catheter, the outer diameter of which was 1.5 mm and the length was 25 mm, was implanted to a depth of 20 mm from the cortex (Fig. 1). After the animals were transferred to a nuclear medical treatment facility, the seed assembly was inserted into the catheter. The catheter was retracted after detention for approximately 7 days such that the total dose at the reference point 8 mm anterior to the midpoint of the radiation source would be 100 Gy. After the catheters were removed, the animals were maintained breeding in the experimental animal facility.

MRI, CT. From 1 week after the completion of the interstitial irradiation, MRI and CT were carried out sequentially at 2 weeks, 1 month, 2 months, 3 months, and 6 months after irradiation. Imaging studies were performed while the animals were under general anesthesia, which was induced by ketamine hydrochloride (10 mg/kg, i.m.) and diazepam (5 mg, i.v.). CT scan was performed using a Yokogawa CT9000 at a thickness of 5 mm, 250 mA and 120 kVp, and in parallel with the line between the infraorbital border and the external auditory canal. Postcontrast CT scanning was performed after intravenous injection of Omnipaque300® (20 ml). A Resona (Yokogawa Medical System, 0.5-tesla) was used for the MRI. Using the same area and thickness as were

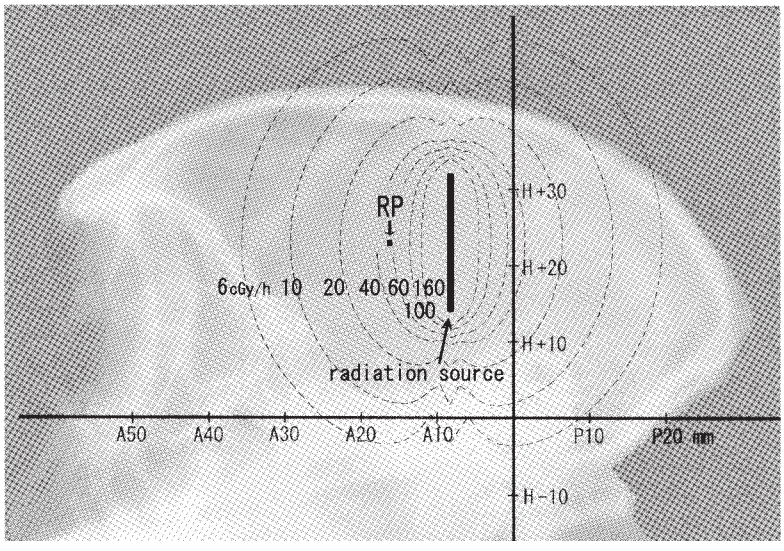

Fig. 1 Radiograph of a monkey skull (lateral view) superimposed on the radiation source and isodose curves; the stereotactic coordinates are shown. The horizontal plane passed through the external auditory meatus and the inferior orbital ridge. The coronal plane passed through both external auditory meatuses. The reference point (RP) was 8 mm anterior to the midpoint of the radiation source.

used for the CT, T_1-weighted images (T_1WI) (TR 600 msec, TE 25 msec, field of view [FOV] 25 cm, 256 × 160 matrix, 4 excitations) with and without enhancement by Gd-DTPA (Magnevist® 4 ml, i.v.), and T_2-weighted images (T_2WI) (TR 2000 msec, TE 100 msec, FOV 25 cm, 256 × 160 matrix, 2 excitations) were taken.

Histological examination. At the end of each observation period (immediately, 1 week, 1 month, 3 months, and 6 months after the end of irradiation), animals were anesthetized with ketamine hydrochloride (10 mg/kg, i.m.) and immobilized with panchronium bromide (0.2 mg/kg, i.m.). They were sacrificed by blood removal and injection of saline from the common carotid artery and the brains were fixed by perfusion with a mixed-solution of 1% glutaraldehyde and 1% paraformaldehyde (0.1 M phosphate buffer, pH 7.4). Then the brains were removed and cut into 5-mm thick slices parallel to the slices on CT and MRI. Each specimen was macroscopically inspected and paraffin-embedded. Then, 6-μm thick sections were made and stained with hematoxylin and eosin (HE), phosphotengustic acid hematoxylin (PTAH), and they were treated using Klüver-Barrera's method; the sections were then inspected through a light microscope.

Results

Survival and neurological changes. Three of the 14 monkeys died within 2 days after the extraction of the radiation source and were excluded from the present experiment. One monkey was sacrificed immediately after treatment, 2 after 1 week, 3 after 1 month, 2 after 3 months, and then 3 after 6 months. Perfusion fixation was performed as mentioned above. All of the animals showed mild left hemiparesis and left hemianopsia. From the 4th to the 9th day after seed implantation (2 to 7 days after the end of irradiation), anorexia was observed, but gradually receded with time. Approximately 2 weeks after the end of irradiation, the symptoms completely disappeared, except for mild left hemiparesis.

Gross findings. Immediately after the end of irradiation until the 1st week, near where the catheter implantation had been, there was some necrosis and a comparatively substantial hemorrhage. Around the necrotic area and hemorrhage, marked edema was observed. Although not shown in the Figure, a cingulate herniation was observed as well. After the 1st month, although the catheter implantation hole did not change, the hemorrhage receded. The necrotic focus expanded and the boundary became clear. The edema in the circumference area became milder. From the 3rd to the 6th month, the hemorrhage completely disappeared, and the necrotic

focus became larger and more distinct (Fig. 2).

Histological findings. Immediately after the end of irradiation to the 1st week (Fig. 3A, B, C), cavitation was observed near the catheter implantation site and the surrounding brain tissue showed coagulative necrosis (CN). Fibrinoid necrosis of vascular walls (arrows: B, C) and exuded fibrin were found around the necrotic focus, as well as bleeding (asterisk: A). Perivascular infiltration of mononuclear cells (arrowheads: B) was observed around the blood vessels.

After the 1st month (Fig. 3D, E, F), cavitation of the catheter insertion area was unchanged and the surrounding tissue showed well demarcated coagulative necrosis (CN). At the periphery of the necrotic focus, abundant lipid-laden macrophages (arrowheads: E) were observed. Using the Kossa method, a positive reaction was recognized inside of the necrotic area, confirming that some calcification, which CT cannot detect, had already occurred. Many reactive astrocytes (arrowheads: F) were observed, as was neovascularization (arrows: F) in the surrounding white matter, but clear fibrinoid necrosis of vascular walls was found only inside of the necrotic area.

From the 3rd to the 6th month (Fig. 3G, H), coagulative necrosis (CN) around the cavity of catheter implantation remained almost the same as at it had been in the 1st month, and xanthoma cells (arrowheads: H) were seen in the circumference. Neovascularization (large arrows: H) caused a further increase in necrosis, and appeared in some areas to be telangiectasia. In addition, some endothelial proliferation and hyalinization of vascular walls (arrows: H) were also observed. Blood vessels that showed fibrinoid necrosis (arrows: G) were seen remaining only inside of the necrosis. The calcareous deposition (large arrowheads: H) became more distinct with time, and was considered to be equivalent to the high-density area seen on the plain CT. In the Table, the pathological changes mentioned above are summarized.

MRI. Around the catheter implantation site, a circular lesion, the inside of which gave low-intensity images, and whose fringe gave relatively high-intensity images, was detected on T_1WI, and the size remained almost the same for 6 months. This lesion matched the necrotic area (discussed above, together with the histological findings). The calculated total dose of the periphery in this area was 200–260 Gy. In the periphery of this circular area, Gd-enhanced T_1WI showed ring enhancement for 6 months. The size of the area was slightly expanded until 3 months after irradiation treatment. The T_2WI images showed a massive high-intensity area in the surrounding white matter, with a midline shift after 1 week. The high-intensity area matched the area of edema; this area shrank to its minimum size after 1 month, and then expanded again after 6 months (Fig. 4).

CT findings. A circular low-density area was observed both on CT and on MRI around the catheter implantation site. Inside the low-density area, a ring-shaped high-density area appeared starting 2 months after irradiation. Six months after irradiation, the high-density area gave a stronger signal. Although this area was not as clearly depicted on CT as it was on MRI, the ring enhancement was seen on the postcontrast CT, as was a low-density area in the surrounding white matter (Fig. 5).

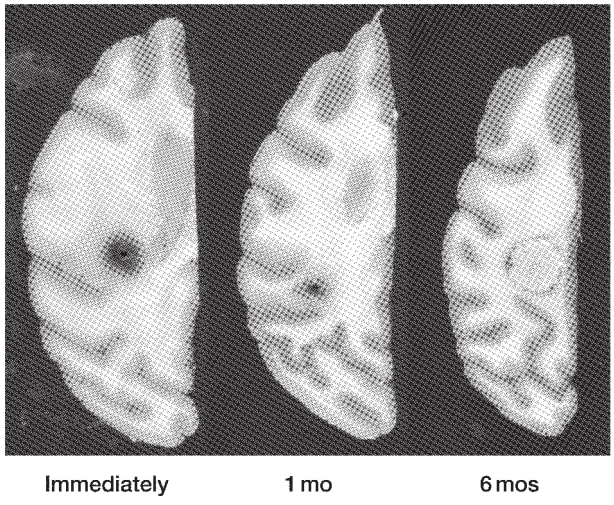

Fig. 2 Horizontal sections on the same plane in MR images and CT scans; immediately (left), 1 month (middle), and 6 months (right) after irradiation. The central necrotic zone gradually became more distinct. Immediately after irradiation (left), the borderline between the gray matter and white matter was unclear. This finding indicated massive edema in the white matter.

Discussion

Radiation injury of normal brain tissues caused by conventional irradiation (external irradiation) is generally classified into 3 categories according to the time of appearance [20, 21]. The first category is for an acute reaction, which occurs during irradiation. This type of injury is thought to be due to an increased intracranial pressure syndrome caused by edema, but it can usually be

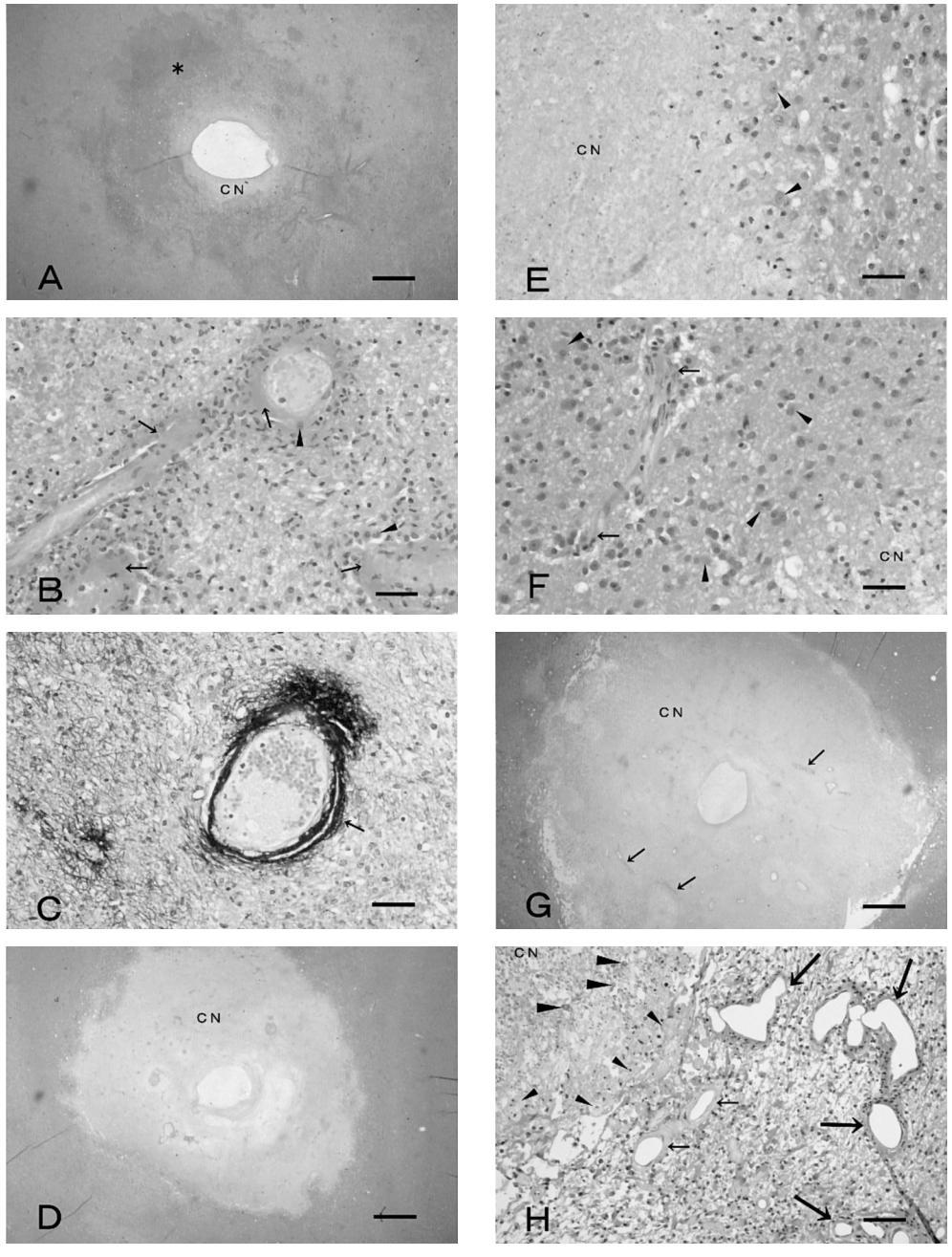

Fig. 3 Photomicrographs of irradiated lesions. Immediately (**A**-**C**), 1 month (**D**-**F**), and 6 months (**G**,**H**) after irradiation. Bars indicate 1mm (**A**,**D**,**G**), 50μm (**B**,**C**,**E**,**F**) and 100μm (**H**). **A**, A central hole and a doughnut-like hemorrhage (asterisk) were seen, and coagulative necrosis (CN) was observed, except for in the central area. HE stain. **B**, Vessels of fibrinoid necrosis (arrows) were seen, and numerous inflammatory cells (arrowheads) had infiltrated the vascular wall and the surrounding brain parenchyma. **C**, Vascular walls of fibrinoid necrosis (arrow) and exuded fibrin were clearly observed. PTHA stain. **D**, Demarcated coagulative necrosis (CN) was clearly observed. HE stain. **E**, Small, scattered calcifications were observed. Around the necrotic area (CN), there was a layer of numerous macrophages (arrowheads). HE stain. **F**, Some neovascularized vessels (arrows) and numerous reactive astrocytes (arrowheads) were observed. HE stain. **G**, The central necrotic zone became clearer, and the vessels of fibrinoid necrosis (arrows) remained within the necrotic area. HE stain. **H**, Many lipid-laden macrophages (arrowheads) and calcareous depositions (large arrowheads) were observed. Some neovascularization (large arrows) and hyalinized vessels (arrows) were found in this area. Granular calcification in the necrotic area, numerous reactive astrocytes, and some degree of edema were observed. HE stain. CN, coagulative necrosis.

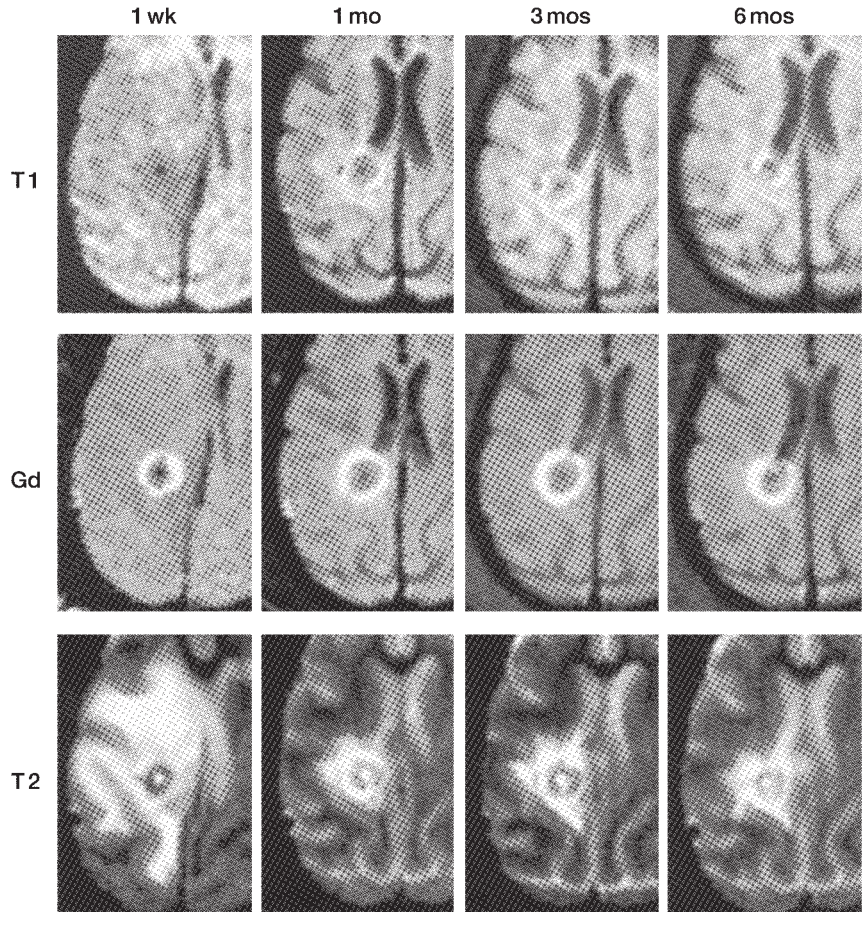

Fig. 4 Serial MR images of a monkey brain 1 week, 1 month, 3 months, and 6 months (left to right) after irradiation. Upper row, T_1WI (T1); middle row, Gd-enhanced T_1WI (Gd); lower row, T_2WI (T2). T_1WI images show a hypointense round lesion from 1 week through 6 months, which was found to be a necrotic zone and was consistently surrounded by a ring enhancement on Gd images. T_2WI showed an extensive hyperintense area outside of the necrotic zone, which demonstrated brain edema. The extent of the edema decreased at 1 month, but it remained for up to 6 months after irradiation.

Table 1 Summary of the histological findings after interstitial irradiation.

	Acute stage (～1 wk)	Subacute stage (1 mo)	Delayed stage (3～6 mos)
Coagulative necrosis	±	++	++
Vessels			
Fibrinoid necrosis	++	+	−～+
Hyalinization	−	+	++
Neovascularization	−～+	+	++
Macrophage	±～+ (perivascular)	+ (peri-necrotic area)	++ (peri-necrotic area)
Calcification	−	+	++
Gliosis	−～+	+++	+++
Edema	++	+	+

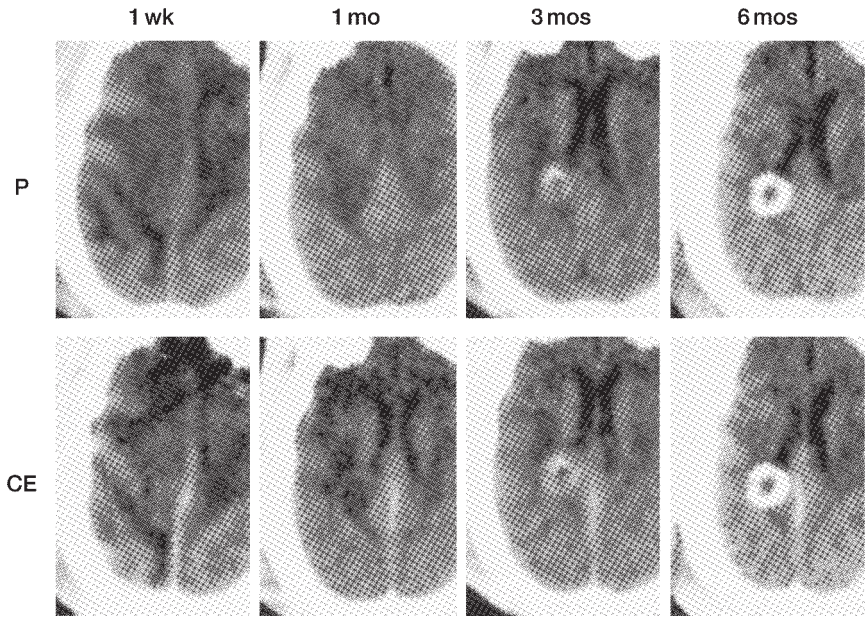

Fig. 5 Serial CT scans of the same monkey as that shown in Fig. 4; 1 week, 1 month, 3 months, and 6 months (left to right) after irradiation. Upper row, precontrast images (P); lower row, post contrast images (CE). Calcification appeared in the necrotic zone at 3 months, and thickened centripetally at 6 months.

managed with corticosteroids [22]. Such symptoms are rarely observed with a total dose of 60 Gy fractionated into 180–200 cGy/day. The second category is for an early delayed reaction that develops after several weeks for up to 2–3 months. This is a disturbance of consciousness caused by demyelination, and in most cases, it naturally disappears after 6 weeks. The third category is for a late delayed reaction, which develops from several months to several years after irradiation. One of its peculiar characteristics is delayed cerebral necrosis, which mainly develops in the white matter, and induces cerebral dysfunction and increased intracranial pressure caused by severe brain edema. This change is irreversible, progressive, and can become fatal in severe cases. It is usually referred to as radiation necrosis and demonstrates an irregular, enhanced mass that may have a necrotic center resembling a recurrent malignant glioma on CT or MRI [23]. This type of radiation necrosis has the following histopathological features: coagulative necrosis, demyelination, macrophagic reaction, perivascular infiltration by inflammatory cells, vascular changes (fibrinoid necrosis, endothelial proliferation, hyaline thickening, capillary telangiectases), and growth of reactive astrocytes [24]. As interstitial brachytherapy is characterized by very high-dose irradiation at the circumference of the radiation source, a steep dose increase in the neighboring tissue, and continuous low-dose irradiation, this type of radiation injury may differ from injuries resulting from conventional external irradiation.

In this experiment using Japanese monkeys, the necrotic focus had distinctive boundaries, and was observed around the catheter implantation site 1 month after the end of irradiation. Strong irradiation is assumed to induce direct cell death; it therefore also causes this necrotic focus, which tended to expand slightly, as seen in the gross and histological findings. However, in the circular area, the presence of a low-intensity core and a relatively high-intensity fringe was observed on the T_1WI of the MRI; this area was thought to correspond to the necrotic focus, and remained almost unchanged in size for 6 months. The total radiation dose at the periphery of this necrotic focus was equivalent to 200–260 Gy. At the center of this necrotic focus, hemorrhage was observed histologically within 2 weeks after the treatment, and gave a very low-intensity signal on T_2WI, due to deoxyhemoglobin 1 week after the treatment. This bleeding was assumed to be caused by direct breakdown of vessel walls because of strong irradiation.

Ostertag *et al.*[16] performed parmanent implantation of iodine-125 seeds into the white matter of beagles, and histologically followed the study at intervals ranging from 25 days to 1 year after implantation. They observed sharply demarcated calcifying necrosis in the area administered more than 180 Gy irradiation, and did not increase in size after 70 days. Fike *et al.* [17] implanted high-activity iodine-125 sources into canine brains from 1 to 10 days, and reported frank coagulative necrosis in the area administered more than 190 Gy irradiation, as shown by CT and histological examination. In addition, Turowski *et al.* [18] left high-activity iodine-125 sources into beagle brains from 1 to 4 days, and observed necrosis in the area administered more than 180–200 Gy irradiation. In the present study, almost the same results were obtained around the necrotic zone.

In the ring enhancement area on MRI surrounding the necrotic focus, fibrinoid necrosis of vessel walls, precipitation of fibrin, and mononuclear cell infiltration were observed at an early stage. Afterward, neovascularization and reactive astrocytes developed in this area. As a mechanism of enhancement on MRI and CT, the extravasation due to disruption of the blood-brain barrier (BBB) and expansion of vascular beds due to neovascularization and telangiectasia-like vascular dilatation could be considered. Many previous reports [25] have suggested that such enhancement is primarily a disruption of the BBB. In the present study, the area in which increased neovascularization and telangiectasia-like findings were observed did not necessarily match the ring enhancement, and therefore the disruption of the BBB was thought to be related to this enhancement.

Groothuis *et al.* [19] executed permanent implantation of iodine-125 seeds into dogs and examined the BBB interruption with ^{14}C-AIB, which was specifically taken up by interrupted sections of the BBB. It was concluded that the BBB interruption had existed for 2 years; it was furthermore assumed that the range of BBB interruption and the K value of ^{14}C-AIB indicating permeability had both remained almost the same throughout the year. It was observed that the K value returned to normal 2 years after the treatment. Fike *et al.* [17] reported that a ring enhancement on CT expanded gradually starting in the second week until the seventh week. In our experiment, the ring enhancement existed for 6 months, and gradually expanded by the third month, thus supporting the results observed by Groothuis and Fikes.

Based on the development of neurological symptoms in this experiment, the edema in the white matter was assumed to be the most prominent 1 week after the end of irradiation. However, according to the MRI findings, the edema shrank gradually until 1 month later, and expanded again in a trend continuing until 6 months after irradiation. Turowski *et al.* [18] observed brain edema on CT, and stated that the most pronounced period of edema was from the 2 nd to the 4th week, and that the edema had disappeared in the 8th week. However, Ostertag *et al.* [16] creported that the edema indicated by immunohistological methods was the most pronounced for a period extended to 120 days; Groothuis *et al.* [19] reported that histologically, the edema appeared to be substantial until 1 year following irradiation, but then had disappeared 2 years following treatment. As regards the necrotic zone and ring enhancement, the results of the present examination were almost the same as those of previous reports, even though the results regarding perifocal edema were completely different. This discrepancy can be attributed to differences in type, strength, and period of placement of the radiation source, as well as to differences in the method of depicting edema. It is already known that the sensitivity of T_2WI of MRI for detecting cerebral lesions outperforms that of CT, because MRI technology is quite sensitive to changes in water content, and also because MRI does not show bone artifacts. As regards radiation injury, many clinical papers [26, 27] have reported that the MRI is more sensitive than CT. Moreover, Gd-enhanced T_1WI clearly demonstrates areas of BBB disruption as high-intensity signals. The advantages of Gd-enhanced MR imaging include the clear display of distinct images, which can be kept for long periods of time. Therefore, T_1WI, T_2WI and Gd-enhanced T_1WI are very important for observing radiation necrosis characterized by blood vessel changes and edema.

From the results of the present study, we speculate that delayed radiation necrosis characterized by long-term coagulative necrosis and perifocal edema is the result of vascular damage. We suggest the schema of radiation injury shown in Fig. 6. In order to clarify the mechanism of normal brain damage caused by interstitial brachytherapy in patients with malignant glioma, longitudinal animal experiments need to be conducted with a focus on dose rate, total dose, and irradiated volume.

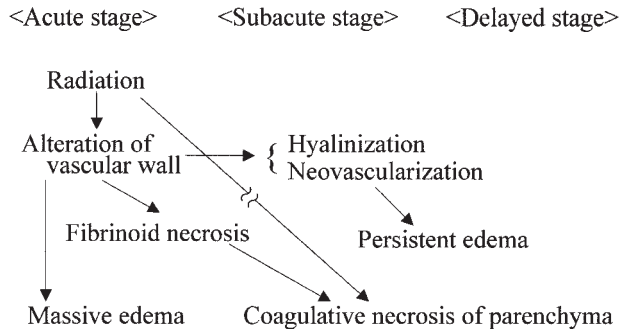

Fig. 6 Schema of radiation injury. During the acute stage, severe irradiation alters the vascular walls to form fibrinoid necrosis, and massive edema is caused by alteration of the vascular walls. At the subacute stage, these vessels contribute to the development of coagulative necrosis of the parenchyma. At the delayed stage, pathologically changed vessels showing features such as hyalinization or neovascularization contribute to persistent edema.

References

1. The committee of brain tumor registry of Japan: Special report of brain tumor registry of Japan (1969–1990). Neurol Med Chir (Tokyo) (1999) 39: 59–107.
2. Bernstein M and Gutin PH: Interstitial irradiation of brain tumors: A review. Neurosurgery (1981) 9: 741–750.
3. Matsutani M: Radiation therapy for malignant gliomas. Jpn J Cancer Chemother (1987) 14: 3219–3226 (in Japanese with English abstract).
4. Bashir R, Hochberg F and Oot R: Regrowth patterns of glioblastoma multiforme related to planning of interstitial brachytherapy radiation fields. Neurosurgery (1988) 23: 27–30.
5. Steiner L, Lindquist C, Cail W, Karlsson B and Steiner M: Microsurgery and radiosurgery in brain arteriovenous malformations. J Neurosurg (1993) 79: 647–652.
6. Prasad D, Steiner M and Steiner L: Gamma surgery for vestibular schwannoma. J Neurosurg (2000) 92: 745–759.
7. Yamanaka K, Iwai Y, Nakajima H, Yasui T, Komiyama M, Nishikawa M, Morikawa T, Kishi H, Negoro S, Tada H and Tanaka M: Treatment for brain metastasis from lung cancer in the era of radiosurgery. No Shinkei Geka (Neurological Surgery) (2001) 29: 617–623 (in Japanese with English abstract).
8. Matsumoto K, Nakagawa T, Tada E, Furuta T, Hiraki Y and Ohmoto T: Effect of adjuvant iridium-192 brachytherapy on the survival of patients with malignant gliomas. Neurol Med Chir (Tokyo) (1997) 37: 891–900.
9. Bakay RAE: Brachytherapy. Contemp Neurosurg (1987) 9: 1–6.
10. Nishio M, Sakurai T, Kagami Y and Narimatsu N: Brachytherapy for cancer. Jpn J Cancer Chemother (1987) 14: 1519–1530 (in Japanese with English abstract).
11. Gutin PH, Leibel SA, Wara WM, Choucair A, Levin VA, Philips TL, Silver P, Da Silva V, Edwards MS, Davis RL, Weaver KA and Lamb S: Recurrent malignant gliomas: Survival following interstitial brachytherapy with high-activity iodine-125 sources. J Neurosurg (1987) 67: 864–873.
12. Bernstein M, Laperriere N, Leung P and McKenzie S: Interstitial brachytherapy for malignant brain tumors: Preliminary results. Neurosurgery (1990) 26: 371–379.
13. Koot RW, Maarouf M, Hulshof MC, Voges J, Treuer H, Koedooder C, Sturm V and Bosch DA: Brachytherapy: Results of two different therapy strategies for patients with primary glioblastoma multiforme. Cancer (2000) 88: 2796–2802.
14. Mishima N, Tomita S, Matsumoto K, Sakurai M, Nakamura S, Nishimoto A, Hiraki Y, Aono K and Taguchi K: A case of recurrent glioma presenting severe brain edema 1.5 months after interstitial brachytherapy. Radiotherapy System Research (1988) Suppl. 5: 170–173 (in Japanese).
15. Csanda E, Komoly S, Takats A and Szucs A: Neuropathological characteristics of beta irradiation induced brain edema. Acta Neuropathol Suppl (Berl) (1981) 7: 67–69.
16. Ostertag CB, Weigel K, Warnke P, Lombeck G and Kleihues P: Sequential morphological changes in the dog brain after interstitial iodine-125 irradiation. Neurosurgery (1983) 13: 523–528.
17. Fike JR, Cann CE, Phillips TL, Bernstein M, Gutin PH, Turowski K, Weaver KA, Davis RL, Higgins RJ and DaSilva V: Radiation brain damage induced by interstitial 125I sources: A canine model evaluated by quantitative computed tomography. Neurosurgery (1985) 16: 530–537.
18. Turowski K, Fike JR, Cann CE, Higgins RJ, Davis RL, Gutin PH, Phillips TL and Weaver KA: Normal brain iodine-125 radiation damage: Effect of dose and irradiated volume in a canine model. Radiology (1986) 158: 833–838.
19. Groothuis DR, Wright DC and Ostertag CB: The effect of 125I interstitial radiotherapy on blood-brain barrier function in normal canine brain. J Neurosurg (1987) 67: 895–902.
20. Leibel SA and Sheline GE: Radiation therapy for neoplasms of the brain. J Neurosurg (1987) 66: 1–22.
21. Matsutani M: Radiation damage to the brain. No To Shinkei (Brain and Nerve) (1987) 39: 694–696 (in Japanese).
22. Tada E, Matsumoto K, Nakagawa M, Tamiya T, Furuta T and Ohmoto T: Serial magnetic resonance imaging of delayed radiation necrosis treated with dexamethasone. Case illustration. J Neurosurg (1997) 86: 1067.
23. Peterson K, Clark HB and Hall WA and Truwit CL: Multifocal enhancing magnetic resonance imaging lesions follwing cranial irradiation. Ann Neurol (1995) 38: 273–344.
24. Rubinstein LJ: Radiation changes in intracranial neoplasms and the adjacent brain; in Tumors of The Cental Nervous System, AFIP, Washington DC (1985) pp 349–360.
25. Valk PE, Budinger TF, Levin VA, Silver P, Gutin PH and Doyle WK: PET of malignant cerebral tumors after interstitial brachytherapy. Demonstration of metabolic activity and correlation with clinical outcome. J Neurosurg (1988) 69: 830–838.
26. Curran WJ, Hecht-Leavitt C, Schut L, Zimmerman RA and Nelson DF: Magnetic resonance imaging of cranial radiation lesions. Int J Radiat Oncol Biol Phys (1987) 13: 1093–1098.
27. Constine LS, Konski A, Ekholm S, McDonald S and Rubin P: Adverse effects of brain irradiation correlated with MR and CT imaging. Int J Radiat Oncol Biol Phys (1988) 15: 319–330.